

# Frozen-in Electrical Field in Thermally Poled Fibers

Danny Wong, Wei Xu, Simon Fleming, Mark Janos,<sup>1</sup> and Kai-Ming Lo<sup>2</sup>

*Australian Photonics Co-operative Research Centre, Optical Fibre Technology Centre, University of Sydney, Australian Technology Park, Eveleigh, New South Wales 1430, Australia*  
E-mail: [d.wong@ofc.usyd.edu.au](mailto:d.wong@ofc.usyd.edu.au)

Received August 5, 1998

---

We have experimentally verified existence of the frozen-in field in thermally poled fiber devices using a Mach–Zehnder interferometer. This technique can be used to measure both the magnitude and the direction of the frozen-in field. This same technique can also be used to measure the third-order nonlinearity  $\chi^{(3)}$  of unpoled fibers and poled fibers. We find out that  $\chi^{(3)}$  of fibers has increased by a factor of  $\sim 2$  after thermal poling.

© 1999 Academic Press

---

## 1. INTRODUCTION

Large linear electro-optic (LEO) coefficients and second-order nonlinearities (SON) in silica fibers and waveguides will make possible many more active fiber and waveguide devices for WDM systems, for example, electro-optic modulators and switches, electrically tunable Bragg gratings and long periodic gratings, electrically tunable filters, frequency converters, and parametric oscillators [1–3]. The creation of  $\chi^{(2)}$  by thermal poling is explained by the establishment of a strong electric field in the anodic region of the thermally poled devices resulting from depletion of positive mobile charges under the applied poling field [4]. Charge distributions in poled glasses were studied by the laser-induced pressure pulse (LIPP) method [5] and the etching technique [6]. It is suggested that there are two layers of space charge: the negatively charged depletion region and the positively charged layer. However, these two methods give neither the direction nor the magnitude of the frozen-in field in poled glasses. Furthermore, it is still not clear

<sup>1</sup> Now with Uniphase Fibre Components.

<sup>2</sup> Now with the University of Hong Kong.

whether  $\chi^{(2)}$  is induced by high d.c. field via  $\chi^{(3)}$  or orientation of dipoles, or a combination of both [7]. This paper addresses these issues.

## 2. EXPERIMENTAL SETUP AND THEORY

A free space Mach–Zehnder interferometer (MZI) operating at 632.8 nm wavelength was used for the measurement of the LEO coefficients in fiber devices, as shown in Fig. 1. Measurements of the magnitudes of modulated signals were taken on the quadrature points of the output of the Mach–Zehnder interferometer. A phase deviation  $\Delta\phi$  about this quadrature point can be calculated from the peak-to-peak amplitude of the measured signal  $\Delta V$  using

$$\Delta\phi = 2 \sin^{-1} \left( \frac{\Delta V}{V_{\max}} \right), \quad (1)$$

where  $V_{\max}$  is the peak-to-peak voltage at the output of the interferometer. From Eq. (1), the electro-optic coefficient  $r$  is calculated using

$$r = \frac{\lambda d}{\pi V_{ac} L n^3} \Delta\phi, \quad (2)$$

where  $\lambda = 632.8$  nm is the free-space optical wavelength of the light,  $V_{ac}$  is a peak-to-peak a.c. testing voltage,  $d$  is the distance between two electrodes,  $n$  is the refractive index of the core, and  $L$  is the length of fiber devices.  $\chi^{(2)}$  is related to  $r$  by the equation [8]

$$\chi^{(2)} = \frac{n^4}{2} r. \quad (3)$$

The fiber devices were made from twin-hole fibers with two fine electrodes threaded into the two holes. In Fig. 2, the electrode in the hole nearer to the core is denoted as the active electrode while the other is denoted as the ground

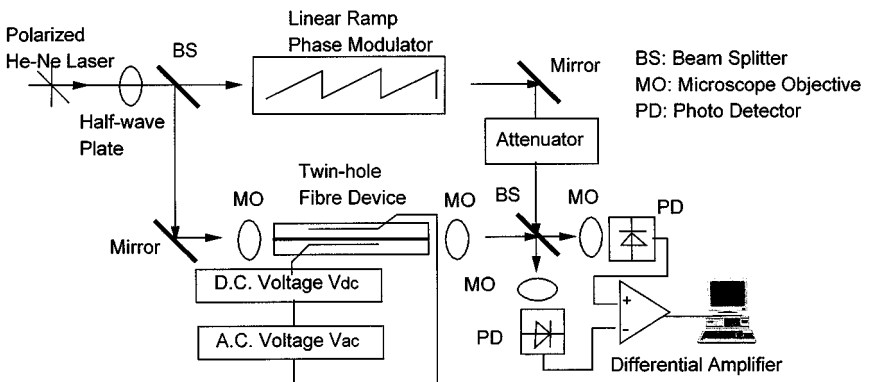
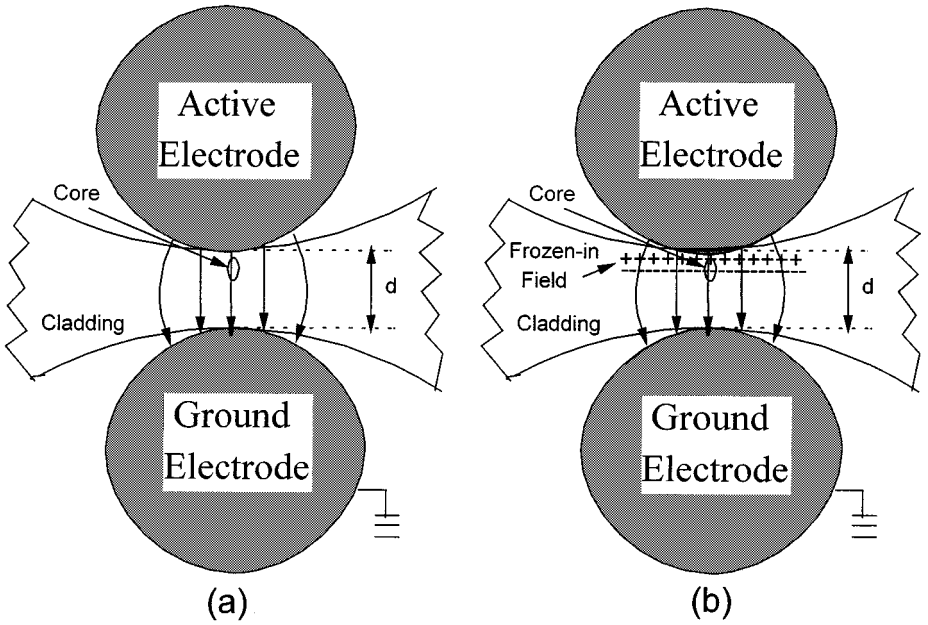


FIG. 1. Experimental setup.



**FIG. 2.** Field distribution for a positive voltage applied to (a) an unpoled fiber device and (b) a poled fiber device with a frozen-in field.

electrode. Either a positive or a negative d.c. voltage, with respect to ground, can be applied to the active electrode for poling. The cross-sectional geometry of the devices and the distribution of the electrical fields in the devices before and after poling are shown in Fig. 2. The solid field lines correspond to a positive d.c. voltage being applied to the active electrode for poling. In Fig. 2b, the frozen-in field formed during poling is shown near to the active electrode. Obviously, a good overlap between the core and the frozen-in field results in a better electro-optic fiber device.

### 3. RESULTS AND DISCUSSION

#### 3.1. Measurement of $\chi^{(3)}$ of Unpoled Fibers

In the experiments, an a.c. testing voltage  $V_{ac}$  of much smaller amplitude ( $\sim 200$  V) was superimposed onto the d.c. voltage  $V_{dc}$ . The linear EO modulation by the  $V_{ac}$  signal was then measured from the output of the MZI. Before poling,  $V_{dc}$  applied to the unpoled devices can cause a second-order nonlinearity [7]

$$\chi^{(2)} = 3\chi^{(3)}E_{dc}, \tag{4}$$

where  $\chi^{(3)}$  is the third-order nonlinearity of the unpoled fiber devices, and  $E_{dc} = V_{dc}/d$ . The electrical field induced linear electric-optic modulation is also well known as electrical field induced second harmonic generation [9]. Combining

Eqs. (2), (3), and (4),  $\chi^{(3)}$  for unpoled fiber devices can be expressed by means of

$$\chi^{(3)} = \frac{n\lambda d^2}{6LV_\pi V_{dc}}, \quad (5)$$

where  $V_\pi$  is the half-wave voltage corresponding to  $V_{dc}$ . As each quantity on the right side of Eq. (5) is measurable, the value of  $\chi^{(3)}$  can be calculated. Figure 3a shows the measured  $\chi^{(2)}$  of an unpoled device as a function of the applied  $V_{dc}$ . It follows from Eq. (4) that  $\chi^{(3)}$  can be estimated from the slope of the plot. For our twin-hole fiber devices, we filled salty ink into two holes in order to get rid of air gaps between the electrodes and the cladding. The value of  $\chi^{(3)}$  for the core of twin-hole fibers is estimated to be  $1.5\text{--}1.86\% \cdot 10^{-22} \text{ (m/V)}^2$ , which is in the same range as  $\chi^{(3)}$  for bulk silica glass of  $1.8\% \cdot 10^{-22} \text{ (m/V)}^2$  [10].  $\chi^{(3)}$  for the core of twin-hole fibers is supposedly larger than  $\chi^{(3)}$  for bulk silica glass due to the existence of germanium in the fiber core.

### 3.2. Frozen-in Field in Thermally Poled Fibers

Fresh devices were poled at +3.5 kV d.c. voltage and at 250°C for ~1 h. After poling, a frozen-in field was induced in the devices. To investigate this frozen-in field in the poled fiber devices, a small a.c. testing voltage  $V_{ac}$  was superimposed onto the d.c. voltage  $V_{dc}$ . Equations (2) and (3) indicate that  $\chi^{(2)}$  is proportional to  $\Delta\phi$ . It can be seen in Fig. 3b that  $\chi^{(2)}$  has a linear dependence on  $V_{dc}$ . We fit the

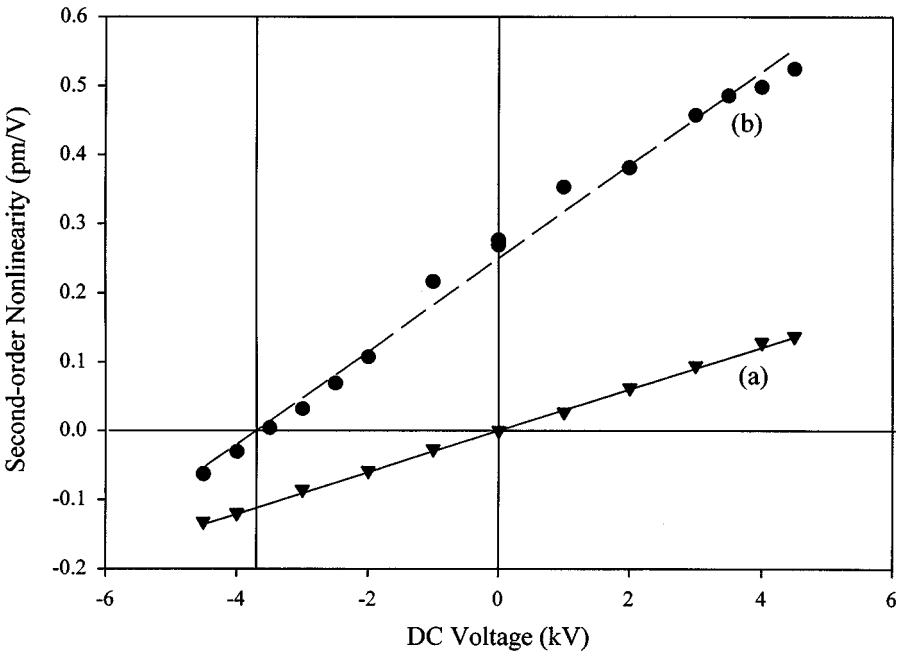


**FIG. 3.** (a) DC-caused  $\chi^{(2)}$  before poling (solid line) and (b) DC-caused  $\chi^{(2)}$  after poling (dash line).

experimental data using the equation

$$\chi^{(2)} = 3\chi_{\text{poled}}^{(3)}E_{\text{dc}} + \chi_{\text{residual}}^{(2)}, \quad (6)$$

where  $\chi_{\text{poled}}^{(3)}$  is the third-order nonlinearity of the poled devices, and  $\chi_{\text{residual}}^{(2)}$  is the residual SON after poling. As shown in Fig. 3b,  $\chi^{(2)}$  became zero when  $-3.7$  kV  $V_{\text{dc}}$  was applied to the poled fiber. This means  $\chi_{\text{residual}}^{(2)}$  was canceled out by the external electrical-field-induced second-order nonlinearity  $\chi_{\text{induced}}^{(2)}$ . Suppose that  $\chi_{\text{residual}}^{(2)}$  is due to the frozen-in field

$$\chi_{\text{residual}}^{(2)} = 3\chi_{\text{poled}}^{(3)}E_{\text{frozen}}; \quad (7)$$

combining Eqs. (6) and (7), we can express the total  $\chi^{(2)}$  of thermally poled fibers as

$$\chi^{(2)} = 3\chi_{\text{poled}}^{(3)}(E_{\text{dc}} + E_{\text{frozen}}). \quad (8)$$

Based on Eq. (8), when the frozen-in field is balanced by the external electrical field, the total  $\chi^{(2)}$  becomes zero. So we can obtain both the magnitude and direction of the frozen-in field in thermally poled fibers. The magnitude of the frozen-in field in this fiber was estimated as  $200$  V/ $\mu\text{m}$ . The direction of the frozen-in field is the same as the direction of the external field caused by the positive  $V_{\text{dc}}$ . The formation of the frozen-in field may be explained as follows. When the fiber device was heated to a temperature of  $\geq 200^\circ\text{C}$ , positive ions in the glass network became mobile and migrated to the cathode under the positive external poling field. The region near to the anode was depleted of positive ions and contained negatively charged centers (layers) embedded in the glass matrix. Due to the short distance between the anode and the negatively charged layers ( $\sim$  a few micrometers), there was a very strong electrical field between them. Ionization took place in the high field at the anodic region, and electrons migrated into the anode. The ionization process created a positively charged layer between the anode and the negatively charged depletion region. The frozen-in field then existed in the area between the positively and negatively charged regions, which was schematically shown in Fig. 2b.

### 3.3. Increase in $\chi^{(3)}$ of Thermally Poled Fibers

Figure 3 shows that the slope of the d.c.-caused EO modulation in the thermally poled fiber is larger than that of the d.c.-caused EO modulation in the unpoled fiber. According to Eqs. (4) and (6), the slopes are proportional to  $\chi^{(3)}$  of the core of twin-hole fibers. This means that the third-order nonlinearity of the poled devices  $\chi_{\text{poled}}^{(3)}$  becomes larger than the third-order nonlinearity of the unpoled devices  $\chi_{\text{unpoled}}^{(3)}$ . The ratio of  $\chi_{\text{poled}}^{(3)}$  to  $\chi_{\text{unpoled}}^{(3)}$  in Fig. 3 is  $\sim 2$ . It follows that a change in material property might have occurred and hence the value of  $\chi^{(3)}$ . In the case of thermal poling, this could be associated with the migration of charges in the glass lattice as well as the redistribution of residual frozen-in thermal stress. In either case, both the material property and the internal field can be changed. It

would be interesting to investigate the relaxation time of these changes. From the microscopic point of view, random dipoles in the glass network are aligned under the frozen-in field. The aligned dipoles could give a higher macroscopic value of  $\chi^{(3)}$  than randomly distributed dipoles. However, the evidence of possible changes in  $\chi^{(3)}$  means that the contribution to  $\chi^{(2)}$  is more than just due to the frozen-in field alone. We are currently including the changes of  $\chi^{(3)}$  in the frozen-in field model for thermal poling of glass fibers.

#### 4. CONCLUSIONS

To our best knowledge, it is believed that this paper is the first to report a method for measuring both the magnitude and the direction of the frozen-in field in thermally poled silica fibers. The value of  $\chi^{(3)}$  for unpoled silica fibers can also be simply obtained using the same measurement technique. The technique is suitable for measuring the third-order nonlinearity of isotropic optical materials. The present results support the frozen-in field model of glass thermal poling and indicates that  $\chi^{(3)}$  of silica fibers has been increased by thermal poling.

#### ACKNOWLEDGMENTS

The authors are grateful for the financial support from the Australian Photonics CRC, ABB, and Transgrid Australia. The author Wei Xu thanks the Department of Employment, Education and Training and Youth Affairs (DEETYA) of the Commonwealth Australia for the Overseas Postgraduate Research Scholarship (OPRS).

#### REFERENCES

- [1] T. Fujiwara, D. Wong, Y. Zhao, S. Fleming, S. Poole, and M. Sceats, "Electro-optic modulation in germanosilicate fibre with UV-excited poling," *Electron. Lett.*, vol. 31, 537 (1995).
- [2] T. Fujiwara, D. Wong, and S. Fleming, "Large electrooptic modulation in a thermally-poled germanosilicate fiber," *IEEE Photon. Technol. Lett.*, vol. 7, 1177 (1995).
- [3] T. Fujiwara, D. Wong, Y. Zhao, S. Fleming, V. Grishina, and S. Poole, "UV-excited poling and electrically tunable Bragg gratings in a germanosilicate fiber," OFC'95 post-deadline paper PD6, San Diego, CA, 1995.
- [4] R. A. Myers, N. Mukherjee, and S. R. J. Brueck, "Large second-order nonlinearity in poled fused silica," *Opt. Lett.*, vol. 16, 1732 (1991).
- [5] P. G. Kazansky, R. A. Smith, P. St. J. Russell, G. M. Yang, and G. M. Sessler, "Thermally poled silica glass: Laser-induced pressure pulse probe of charge-distribution," *Appl. Phys. Lett.*, vol. 68, 269 (1996).
- [6] W. Margulis and F. Laurell, "Interferometric study of poled glass under etching," *Opt. Lett.*, vol. 21, 1786 (1996).
- [7] P. G. Kazansky and V. Pruneri, "Fundamentals of glass poling: From self-organization to electric-field poling," in *Bragg Gratings, Photosensitivity, and Poling in Glass Fibres and Waveguides: Applications and Fundamentals*, Virginia, Paper BtuC6, pp. 305–307, 1997.

- [8] B. E. A. Saleh and M. C. Teich, *Fundamentals of Photonics*, Chap. 19, pp. 740–746, Wiley, New York (1991).
- [9] D. Statman and J. A. Georges III, “Charge dynamics and poling in glass waveguides,” *J. Appl. Phys.*, vol. 80, 654 (1996).
- [10] R. Adair, L. L. Chase, and S. A. Payne, “Nonlinear refractive-index measurements of glasses using three-wave frequency mixing,” *J. Opt. Soc. Am. B*, vol. 4, 875 (1987).